ACCURACY OF THREE UNCONDITIONALLY-STABLE FDTD SCHEMES FOR SOLVING MAXWELL'S EQUATIONS

Guilin Sun and Christopher W. Trueman

Electromagnetic Compatibility Laboratory, Concordia University,
7141 Sherbrooke Street West, Montreal, Quebec, Canada H4B 1R6

Abstract - **This paper discusses accuracy limitations due to numerical dispersion and time step size for three implicit unconditionally-stable FDTD methods: Alternate-Direction-Implicit (ADI), Crank-Nicolson (CN) and Crank-Nicolson-Douglas-Gunn (CNDG). It is shown that for a uniform mesh, the three methods have the same numerical phase velocity along the axes, but have large differences along the diagonals. The ADI method has two orders-of-magnitude larger anisotropy than that of CN and CNDG. CNDG has no anisotropy at certain Courant numbers and mesh densities. At the limit of zero spatial mesh size, the three methods have different "intrinsic temporal dispersion" for a given time step size: CN has no anisotropy; ADI has positive anisotropy and CNDG has negative anisotropy, which is much smaller than ADI. The Nyquist sampling theorem provides a fundamental upper bound on the time step size for all three methods. It is shown that for ADI and CN the practical upper bound is close to the Nyquist limit, but for CNDG is half the Nyquist limit.**

Keywords - **Maxwell's Equations, Finite-difference time-domain method, Alternate-Direction-Implicit method, Crank-Nicolson method, Douglas-Gunn method, numerical dispersion, numerical anisotropy, accuracy, Nyquist criterion.**

I. Introduction

Yee's Finite-Difference Time-Domain (FDTD) method is popular for solving Maxwell's Equations [1]. It is second-order accurate in both time and space [2]. Since it is an explicit method [3], it is easy to program and efficient to run. However it suffers from the Courant-Friedrich-Levy (CFL) limit or the Courant limit on the time step size required for stability. For objects with fine geometrical features, using a fine mesh size greatly reduces the allowable time step size, which causes the CPU time to be prohibitively long. To eliminate the CFL limit, unconditionally-stable methods working with large Courant numbers are desirable. Early in 1984, Holland [4] proposed an implicit method but it was not completely stable. In 1995, Shang [5] developed an efficient characteristic-based algorithm and Fijany [6] proposed a parallel Crank-Nicolson (CN) method by decomposition of the eigenvalue/eigenvector for the wave equations of the second order. In 1999 and 2000, Namiki [7] and Zhen et al. [8] suggested an Alternate-Direction-Implicit (ADI) method. In 2001, Beggs and Briley [9] reported a two-factor scheme by combining a characteristic-based approach to spatial differencing with an implicit lower-upper approximate factorization that avoids the solution of a tridiagonal system. Very recently, Sun and Trueman [10] proposed a Crank-Nicolson scheme with Douglas-Gunn algorithm (CNDG).

This paper compares the numerical dispersion and anisotropy of the ADI, CN and CNDG methods used in FDTD, and analyzes some of their common characteristics and differences. For simplicity, Yee's mesh [1] in 2D is used with a TE_z wave in a linear, isotropic, non-dispersive and lossless medium. This paper is organized as follows. In Section II, the amplification factors are listed for the three methods. In Section III, their numerical dispersion relations are given and compared for a given mesh density. In Section IV their numerical anisotropy is analyzed and compared at different Courant numbers. In Section V the time step size limits are discussed and related to the Nyquist criterion. In Section VI the accuracy limit due to dispersion is analyzed for zero spatial mesh size.

II. Amplification Factors

The update equations for the ADI-FDTD, CN-FDTD and CNDG-FDTD methods are listed in Appendices. The ADI-FDTD uses two sub-steps [7] (Appendix I). The first sub-step advances time from step n to step n+1/2. The field component $E_y^{n+1/2}$ is fully implicit and requires solving a tridiagonal matrix. The second sub-step advances time step from n+1/2 to n+1, and the field component E_x^{n+1} is fully implicit and also requires solving a similar tridiagonal matrix. The time step n+1/2 is intermediate and the field values at this step are non-physical. The amplification factors for the two sub-steps are [7,11]

$$\xi_1 = \sqrt{\frac{1+r_y^2}{1+r_x^2}}\, e^{-j\tan^{-1}((1+r_x^2)(1+r_y^2)-1)} \tag{1}$$

$$\xi_2 = \sqrt{\frac{1+r_x^2}{1+r_y^2}}\, e^{-j\tan^{-1}((1+r_x^2)(1+r_y^2)-1)} \tag{2}$$

where $j=\sqrt{-1}$, $r_x = c\Delta t \sin(\beta_x \Delta_x / 2)/\Delta_x$, $r_y = c\Delta t \sin(\beta_y \Delta_y / 2)/\Delta_y$, Δt is the time step size, $c = 1/\sqrt{\mu\varepsilon}$ is the physical velocity, ε and μ are the permittivity and permeability of the material respectively, Δx and Δy are the spatial meshing sizes along x and y axes; $\beta_x = \beta\cos(\phi)$, $\beta_y = \beta\sin(\phi)$, $\beta^2 = \beta_x^2 + \beta_y^2$ where β is the numerical wave phase constant; and angle ϕ is the direction of travel with respect to the x axis.

The CN scheme averages the field components at time step n and n+1 to maintain second order accuracy in time [6, 10] (Appendix II). It has no intermediate time step. But the resulting block tridiagonal matrix is very expensive to solve by direct methods such as the Gaussian elimination or the banded matrix method, as well as by iterative methods such as Successive Over-Relaxation (SOR) or the iterative Alternate-Direction-Implicit (IADI) method [3]. Since the discretization of the Poisson Equation and heat equation also leads to such a block tridiagonal matrix, several other methods to solve it can be found in Refs. [3] and [12]. Finjany et al. [6] solve the block tridiagonal matrix by eigenvalue/eigenvector decomposition.

Different solution methods for the block tridiagonal matrix may have different amplification factors and different numerical dispersion relations. This paper assumes a direct solution method of the block tridiagonal matrix such as the Gaussian elimination for the CN-FDTD method. The amplification factor for this CN method is [10]

$$\xi_{CN} = e^{\pm j \tan^{-1}\left(\frac{\sqrt{(1+r_x^2+r_y^2)^2-(1-r_x^2-r_y^2)^2}}{1-r_x^2-r_y^2}\right)} \tag{3}$$

Note that the magnitude of the amplification factor for the CN method is unity.

The CNDG method avoids an expensive direct solution (Appendix III). It factorizes the block tridiagonal matrix and has two sub-steps: the first sub-step finds the intermediate field value H_z^*, and the second sub-step gets the solution at the time step n+1 [10]. Thus, like the ADI method, the CNDG method needs to solve a tridiagonal matrix at each sub-step. The amplification factor is

$$\xi_{CNDG} = e^{\pm j \tan^{-1}\left(\frac{\sqrt{(1+r_x^2)^2(1+r_y^2)^2-(1-r_x^2)^2(1-r_y^2)^2}}{(1-r_x^2)(1-r_y^2)}\right)} \tag{4}$$

Though ADI and CNDG both have two sub-steps, there are some differences. In CNDG, the time level of the intermediate step is unknown, and there is only one amplification factor for the two sub-steps, of unity magnitude. On the other hand, in ADI, the intermediate time is $(n+1/2)\Delta t$, and each sub-step has its own amplification factor. The magnitudes of the two amplification factors for the two individual sub-steps are reciprocals. Their product is the magnitude of the amplification factor for one full update cycle, and is unity. Note that the unity magnitude of the amplification factors ensures that the three implicit methods are unconditionally stable and strictly non-dissipative.

III. Numerical Dispersion

The numerical dispersion relation can be written for the three methods [10, 11] as

$$\tan^2(\omega\Delta t/2) = r_x^2 + r_y^2 + g r_x^2 r_y^2 \tag{5}$$

where the factor g is

$$g = \begin{cases} 1 & ADI \\ 0 & CN \\ -\tan^2(\omega\Delta t/2) & CNDG \end{cases} \tag{6}$$

Given a frequency ω, a mesh size Δx and Δy, a time step size Δt, and direction of travel ϕ, Eqn. (5) is solved implicitly for the phase constant β. For a wave to propagate β must be real. The numerical dispersion is quantified by the relative velocity that is defined as the ratio of the numerical velocity to the physical velocity.

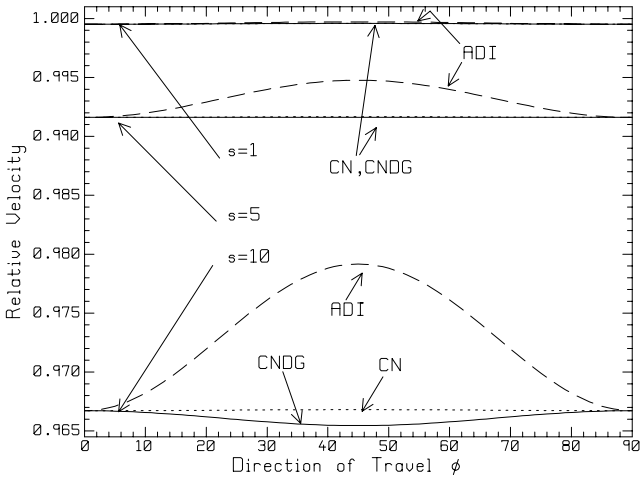

Fig. 1 Numerical dispersion with mesh density 100 and s=1, 5 and 10, for ADI, CN and CNDG.

The numerical dispersion relation in Eqn. (5) for the ADI and CNDG methods has been validated with numerical experiments [10,11]. Fig.1 shows the relative velocity as a function of the direction of travel, using

$\Delta x = \Delta y$ with mesh density $N = 100$ cells per wavelength, at different Courant numbers $s = c\Delta t / \Delta x$ equal to 1, 5 and 10. Note that the numerical dispersion curves of the CN method and the CNDG method are almost identical, and are difficult to distinguish visually in Fig.1. The relative velocity along the axes is exactly the same for the three methods, but along the diagonal ADI is quite different from CN or CNDG. Thus their numerical anisotropies are significantly different, which will be discussed in the next section.

The "grid-related numerical dispersion" is defined as the dispersion at zero time step size. Since the cross term $gr_x^2 r_y^2$ in Eqn. (6) goes to zero as time step size approaches zero, the grid-related numerical dispersion is the same for the three methods, and is the same as that of Yee's FDTD [2, 13].

IV. Numerical Anisotropy

The velocity-anisotropy error is often used to quantify the numerical anisotropy [2]. In an isotropic medium, the wavefront of a cylindrical wave is a circle, that is, the phase velocity is the same in all directions. However, in the numerical domain, the numerical wave velocity usually depends on the direction of travel. Like Yee's FDTD with a uniform mesh, the ADI and CN methods have the largest velocity along the diagonals and slowest along the axes, as shown in Fig. 1.

However, the CNDG behaves differently from CN or ADI. At certain combinations of the mesh and time step sizes, the velocity u_{45° along the diagonals can be slower than the velocity u_{0° along the axes. To evaluate this phenomenon, the following definition of the velocity anisotropy is used for a uniform mesh

$$\Delta u = \frac{u_{45^\circ} - u_{0^\circ}}{\min\{u_{45^\circ}, u_{0^\circ}\}} \times 100\% \qquad (7)$$

This error definition has the same magnitude as that Taflove and Hagness [2], but can be positive or negative, depending on which velocity is larger. Fig. 2 and Fig. 3 show the numerical anisotropy at mesh densities from 50 to 100 cells per wavelength for the ADI, CN and CNDG methods. The anisotropy of ADI is about two orders of magnitude larger than that of CN and CNDG. As the Courant number increases, the anisotropy in ADI increases significantly. The CN and CNDG have the same behaviour. For the Courant number smaller than about 11, the anisotropy of CNDG is always smaller than that of CN; for the Courant number larger than 11, the anisotropy of CNDG is larger than that of CN at coarse mesh density (for example, 50), but it quickly becomes smaller than that of CN after certain mesh densities. For instance, if the Courant number is 12, at the mesh density 50, the numerical anisotropy is –0.148*0.01 for CNDG and 0.082*0.01 for CN; at mesh density 55, their absolute anisotropy values are the same, about 0.066*0.01. However, at mesh density 60, CN has 0.055*0.01 but CNDG has only 0.038*0.01.

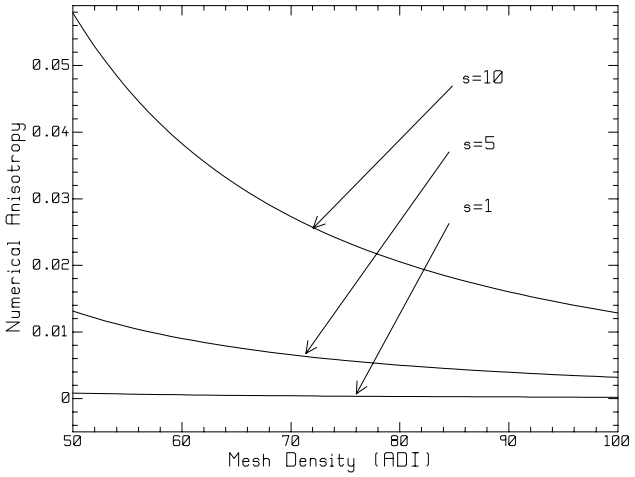

Fig. 2 Numerical anisotropy of the ADI method at Courant numbers 1,5 and 10.

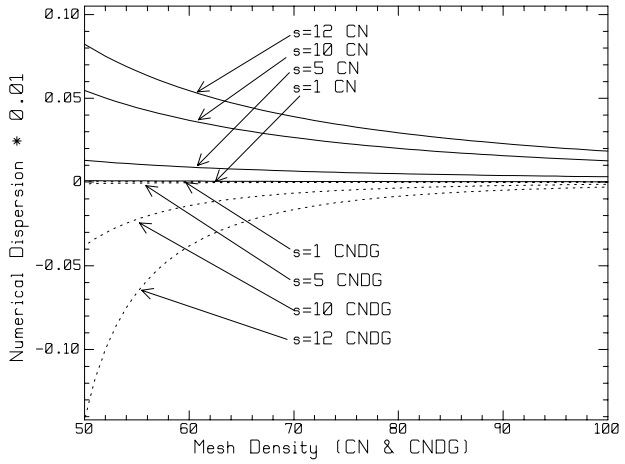

Fig. 3 Numerical anisotropy for CN and CNDG.

Notice that the anisotropy changes its sign for CNDG at certain combinations of the mesh density and Courant number. This suggests that at certain Courant numbers, a mesh may have no anisotropy. Fig. 4 shows the relation between the Courant number and mesh density with zero anisotropy. Note that neither ADI nor CN has this behavior.

V. Time Step Size Limitations

In the numerical dispersion relation of Eqn. (5), if the tangent is infinite, the phase constant becomes complex for all the three methods. This limit is reached when

$$\Delta t = \frac{1}{2f} \qquad (8)$$

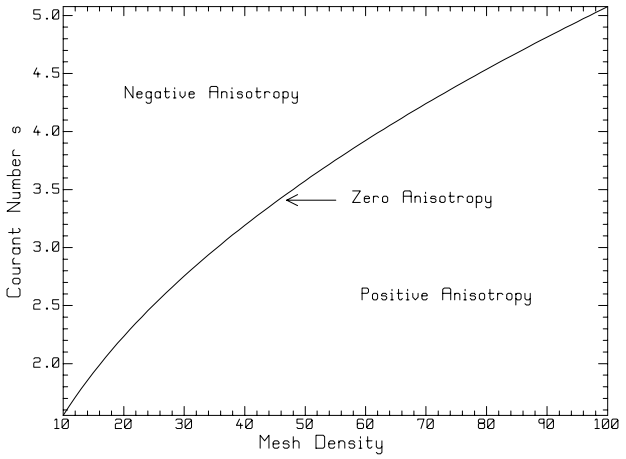

Fig. 4 The relation of the Courant number and mesh density at zero anisotropy for CNDG.

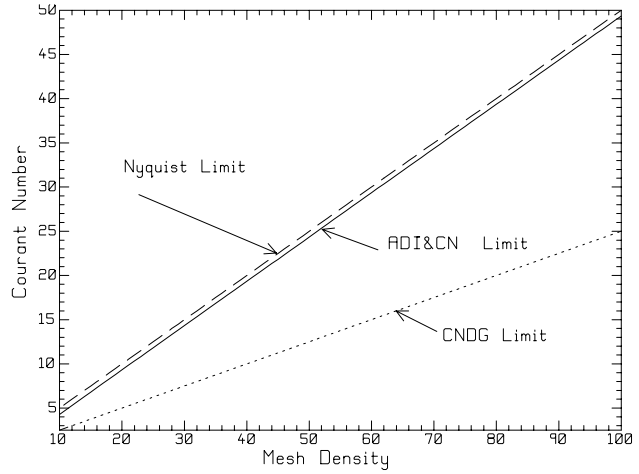

Fig. 5 Time step size limits with respect to mesh density for the three methods.

Eqn. (8) is recognized as the Nyquist limit for the time sampling. For a given mesh density *N*, the Nyquist limit can be written in relation to the Courant number as

$$s = \frac{N}{2} \tag{9}$$

However, Eqn. (5) implies a smaller time step size limit than the Nyquist limit. For example, along the *x*-axis, $\sin(\beta\Delta x/2)$ must be smaller than or equal to one if β is to be real. For the ADI and CN methods, the minimum velocity always occurs along the axes, so the limiting Courant number for a give mesh density can be found from Eqn. (5) to satisfy $\tan(\pi s/N) = s$. For the CNDG method, at larger Courant numbers, the minimum velocity is along the diagonals. For $\Delta x = \Delta y$, Eqn. (5) for the CNDG method leads to

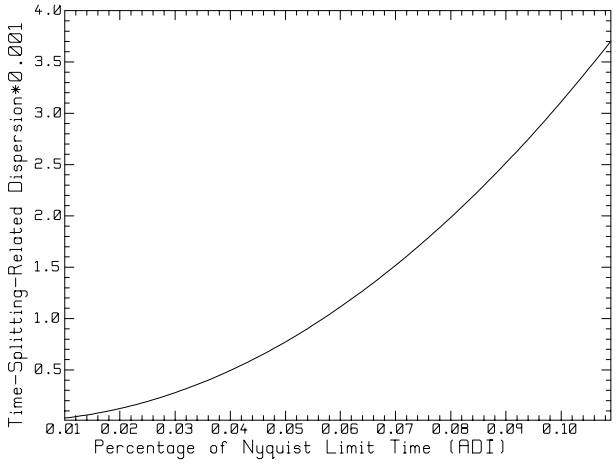

Fig. 6 Intrinsic temporal anisotropy with zero mesh size for ADI.

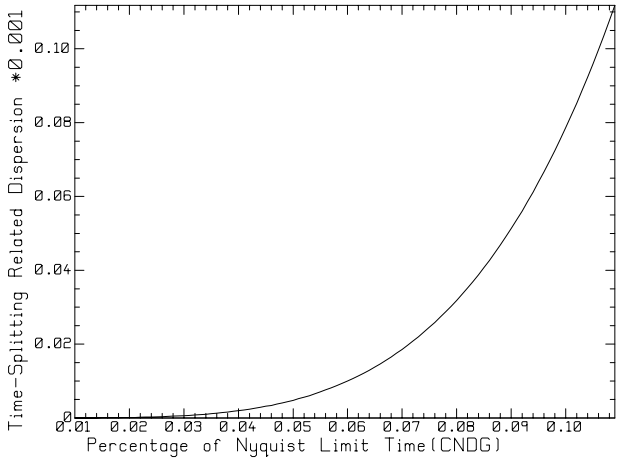

Fig. 7 Intrinsic temporal anisotropy with zero mesh size for CNDG.

$$\sin^2(\sqrt{2}\beta_{45^\circ}\Delta x/4) = \frac{1+\sqrt{1-\tan^4(\omega\Delta t/2)}}{(s\tan(\omega\Delta t/2))^2} \tag{10}$$

where β_{45° is the phase constant along the diagonals. If $\tan(\omega\Delta t/2) > 1$, then the phase constant β becomes a complex number. Thus $\tan(\omega\Delta t/2) = 1$ is the limit for the CNDG method. This corresponds to $s = N/4$. The three curves shown in Fig. 5 are the Nyquist limit, and the step size limits for the ADI and CN methods and for the CNDG method. If a method uses a Courant number larger than its limit shown in Fig. 5, numerical attenuation will occur, which does not correspond to the physical reality.

VI. Intrinsic Temporal Dispersion

In Yee's FDTD, as the mesh density increases, the numerical dispersion decreases. In the limit of an

infinitely-fine mesh, that is, zero spatial mesh size, there is no numerical dispersion because the Courant limit forces the time step size to be zero. Hence, Yee's method collapses to the continuous case, that is, no discretization for time and space. But for the unconditionally-stable implicit methods, because there is no Courant limit, fine mesh size can be accompanied by very large time step size and the method remains stable. Even in the limit of zero spatial mesh size, the methods are still stable for any time step size, but there is numerical dispersion. The numerical dispersion at zero mesh size is an intrinsic limitation and may be termed "intrinsic temporal dispersion", previously called "time-splitting-related dispersion" [11]. The intrinsic temporal dispersion is different for the three methods. With some manipulation, it can be written as

$$\frac{u}{c} = \frac{\omega\Delta t/2}{\tan(\omega\Delta t/2)}\sqrt{\frac{1+\sqrt{1+g(\tan(\omega\Delta t/2)\sin 2\phi)^2}}{2}} \tag{11}$$

Numerical calculations using Eqn. (11) show that the intrinsic temporal dispersion as a function of the direction of travel is similar to that shown in Fig. 1 but smaller in magnitude. From Eqn. (11) it can be seen that the relative velocity is not a function of direction of travel for the CN method. Therefore CN's anisotropy is zero at the zero mesh size limit. But for ADI and CNDG, there is anisotropy, as shown in Fig. 6 and Fig. 7. This anisotropy is termed the "intrinsic temporal anisotropy." Note that the ADI's anisotropy is about 30 times larger than that of CNDG at the time step size of one-tenth Nyquist time step size limit.

Note that in Eqn. (11) the tangent cannot be larger than unity for CNDG method; otherwise the velocity will be a complex number. This time step size limit corresponds to

$$\Delta t\Big|_{CNDG} = \frac{1}{2}\frac{1}{2f} \tag{12}$$

This is half of the Nyquist limit, and coincides with that in Section V for the time step size limit of the CNDG method. For non-zero mesh size, the numerical velocity is always smaller than the intrinsic temporal dispersion, therefore Eqn. (11) is a fundamental accuracy limit for the three methods.

VII. Conclusion

This paper has discussed several aspects of the ADI, CN and CNDG methods. The magnitude of the overall amplification factor for all three methods is unity; hence they are all unconditionally stable. The numerical dispersion is the same along the axes for the three methods, but differs along the diagonals. The anisotropy in the ADI method is two orders-of-magnitude larger than that of CN and CNDG. In the limit of zero mesh size, ADI and CNDG have anisotropy but the CN method does not. Different from the ADI and CN methods, the CNDG method may have slower velocity along the diagonals than along the axes, and may have zero anisotropy at certain combinations of Courant number and mesh density. The three methods have time step size limits that are smaller than the Nyquist criterion. CNDG has the smallest time step limit. The intrinsic temporal dispersion is a fundamental accuracy limit for the three methods and is much larger for ADI than for CN or CNDG along the diagonals.

APPENDIX I Update Equations for ADI-FDTD

The ADI-FDTD has two sub-steps. The first sub-step is advancing time from step n to step n+1/2 by use of the following update equations [7]

$$E_x^{n+1/2}(i+1/2,j) = E_x^n(i+1/2,j) + a_1\{ H_z^n(i+1/2,j+1/2) - H_z^n(i+1/2,j-1/2)\}/\Delta y \tag{I-1}$$

$$E_y^{n+1/2}(i,j+1/2) = E_y^n(i,j+1/2) - a_1\{ H_z^{n+1/2}(i+1/2,j+1/2) - H_z^{n+1/2}(i-1/2,j+1/2)\}/\Delta x \tag{I-2}$$

$$H_z^{n+1/2}(i+1/2,j+1/2) = H_z^n(i+1/2,j+1/2) + a_2\{ E_x^n(i+1/2,j+1) - E_x^n(i+1/2,j)\}/\Delta y - a_2\{E_y^{n+1/2}(i+1,j+1/2) - E_y^{n+1/2}(i,j+1/2)\}/\Delta x \tag{I-3}$$

where $a_1 = \Delta t/2\varepsilon$, $a_2 = \Delta t/2\mu$, Δt is the time step size; ε and μ are the permittivity and permeability of the material respectively; Δx and Δy are the spatial meshing sizes along x and y axes; i and j are the integer-number indices of the computational cells; and n is the time step index. In this step, $E_y^{n+1/2}$ is implicit and can be found by solving a tridiagonal matrix of the form

$$E_y^{n+1/2}(i-1,j+1/2) - \{(\Delta x^2/a_1a_2 + 2)E_y^{n+1/2}(i,j+1/2) + E_y^{n+1/2}(i+1,j+1/2) = -(\Delta x^2/a_1a_2)E_y^n(i,j+1/2) + (\Delta x/a_2)\{H_z^n(i+1/2,j+1/2) - H_z^n(i-1/2,j+1/2)\} + \Delta x/\Delta y\{E_x^n(i+1/2,j+1) - E_x^n(i+1/2,j) + E_x^n(i-1/2,j) - E_x^n(i-1/2,j+1)\} \tag{I-4}$$

The second sub-step advances time step from n+1/2 to n+1 and the update equations are

$$E_x^{n+1}(i+1/2,j)=E_x^{n+1/2}(i+1/2,j)+a_1\{ H_z^{n+1}(i+1/2,j+1/2)-H_z^{n+1}(i+1/2,j-1/2)\}/\Delta y \quad \text{(I-5)}$$

$$E_y^{n+1}(i,j+1/2)=E_y^{n+1/2}(i,j+1/2)-a_1\{ H_z^{n+1/2}(i+1/2,j+1/2)-H_z^{n+1/2}(i-1/2,j+1/2)\}/\Delta x \quad \text{(I-6)}$$

$$H_z^{n+1}(i+1/2,j+1/2)=H_z^{n+1/2}(i+1/2,j+1/2)+a_2\{ E_x^{n+1}(i+1/2,j+1)-E_x^{n+1}(i+1/2,j)\}/\Delta y - a_2\{E_y^{n+1}(i+1,j+1/2)-E_y^{n+1}(i,j+1/2)\}/\Delta x \quad \text{(I-7)}$$

Since E_x^{n+1} is implicit and it is found by solving a tridiagonal matrix of the form

$$E_x^{n+1}(i+1/2,j-1)-\{\Delta y^2/a_1a_2+2)E_x^{n+1}(i+1/2,j)+ E_x^{n+1}(i+1/2,j+1)=-(\Delta y^2/a_1a_2)E_x^{n+1/2}(i+1/2,j)+ (\Delta y/a_2)\{H_z^{n+1/2}(i+1/2,j-1/2)- H_z^{n+1/2}(i+1/2,j+1/2)\} + \Delta y/\Delta x\{E_y^{n+1/2}(i+1,j+1/2)-E_y^{n+1/2}(i,j+1/2)+ E_y^{n+1/2}(i+1,j-1/2)-E_y^{n+1/2}(i,j-1/2)\} \quad \text{(I-8)}$$

APPENDIX II Update Equations for CN-FDTD

The CN scheme averages the field components at time step n and n+1 to maintain second order accuracy in time as follows [6, 10]

$$E_x^{n+1}(i+1/2,j)=E_x^n(i+1/2,j)+ a_1\{H_z^{n+1}(i+1/2,j+1/2)-H_z^{n+1}(i+1/2,j-1/2)+ H_z^n(i+1/2,j+1/2)-H_z^n(i+1/2,j-1/2)\}/\Delta y \quad \text{(II-1)}$$

$$E_y^{n+1}(i,j+1/2)=E_y^n(i,j+1/2)- a_1\{H_z^{n+1}(i+1/2,j+1/2)-H_z^{n+1}(i-1/2,j+1/2)+ H_z^n(i+1/2,j+1/2)-H_z^n(i-1/2,j+1/2)\}/\Delta x \quad \text{(II-2)}$$

$$H_z^{n+1}(i+1/2,j+1/2)=H_z^n(i+1/2,j+1/2)+ a_2\{E_x^{n+1}(i+1/2,j+1)-E_x^{n+1}(i+1/2,j)+ E_x^n(i+1/2,j+1)-E_x^n(i+1/2,j)\}/\Delta y- a_2\{E_y^{n+1}(i+1,j+1/2)-E_y^{n+1}(i,j+1/2)+ E_y^n(i+1,j+1/2)-E_y^n(i,j+1/2)\}/\Delta x \quad \text{(II-3)}$$

The block tridiagonal matrix to be solved for the CN method is

$$H_z^{n+1}(i+1/2,j+1/2)-a_1a_2\{H_z^{n+1}(i+3/2,j+1/2)+ H_z^{n+1}(i-1/2,j+1/2)-2H_z^{n+1}(i+1/2,j+1/2\}/\Delta x^2 - a_1a_2\{H_z^{n+1}(i+1/2,j+3/2)+H_z^{n+1}(i+1/2,j-1/2)- 2H_z^{n+1}(i+1/2,j+1/2)\}/\Delta y^2= H_z^n(i+1/2,j+1/2)+a_1a_2\{H_z^n(i+3/2,j+1/2)+ H_z^n(i-1/2,j+1/2)-2H_z^n(i+1/2,j+1/2)\}/\Delta x^2 + a_1a_2\{H_z^n(i+1/2,j+3/2)+H_z^n(i+1/2,j-1/2)- 2H_z^n(i+1/2,j+1/2)\}/\Delta y^2 + 2a_2\{[E_x^n(i+1/2,j+1)-E_x^n(i+1/2,j)/\Delta y-]- [E_y^n(i+1,j+1/2)-E_y^n(i,j+1/2)]/\Delta x\} \quad \text{(II-4)}$$

APPENDIX III Update Equations for CNDG-FDTD

The update equations of CNDG-FDTD are the same as the CN method. The difference between the CN-FDTD and CNDG-FDTD is the method used to solve the block tridiagonal matrix. In CNDG-FDTD, it is factorized into two sub-steps [10]

$$H_z^*(i+1/2,j+1/2)-a_1a_2\{H_z^*(i+3/2,j+1/2)+ H_z^*(i-1/2,j+1/2)-2H_z^*(i+1/2,j+1/2)\}/\Delta x^2 = H_z^n(i+1/2,j+1/2)+a_1a_2\{H_z^n(i+3/2,j+1/2)+ H_z^n(i-1/2,j+1/2)-2H_z^n(i+1/2,j+1/2)\}/\Delta x^2 + a_1a_2\{H_z^n(i+1/2,j+3/2)+H_z^n(i+1/2,j-1/2)- 2H_z^n(i+1/2,j+1/2)\}/\Delta y^2 + 2a_2\{[E_x^n(i+1/2,j+1)-E_x^n(i+1/2,j)]/\Delta y- [E_y^n(i+1,j+1/2)-E_y^n(i,j+1/2)]/\Delta x\} \quad \text{(III-1)}$$

$$H_z^{n+1}(i+1/2,j+1/2)-a_1a_2\{H_z^{n+1}(i+1/2,j+3/2)+ H_z^{n+1}(i+1/2,j-1/2)-2H_z^{n+1}(i+1/2,j+1/2)\}/\Delta y^2 = H_z^*(i+1/2,j+1/2) \quad \text{(III-2)}$$

At each sub-step a tridiagonal matrix must be solved. It can be seen that the ADI method solves the electric fields implicitly, but the CN and CNDG methods solve the magnetic field implicitly in the 2D TE_z case.

REFERENCES

[1] K.S., Yee, "Numerical solution of initial boundary value problems involving Maxwell's equations in isotropic media," IEEE Trans. Antennas and Propagation, Vol.14, May, 1966, pp. 302-307.

[2] A.,Taflove, and S.C., Hagness, *Computational electrodynamics—the finite-difference time-domain method*, 2nd ed., Artech House, Boston, 2000.
[3] J.Stoer, R.Bulirsch, "Introduction to numerical analysis," 3rd ed, Translated by R.Bartels, W. Gautschi and C.Witzgall, Springer-Verlag, New York, 2002.
[4] R.Holland, "Implicit three-dimensional finite differencing of Maxwell's equations for computational electromagnetism," IEEE Trans. Nucl. Sci., Vol.NS-31, 1984, pp. 1322-1326.
[5] J. S. Shang, "A fractional-step method for solving 3D, time-domain Maxwell Equations," J. of. Comput. Phys., Vol. 118, 1195, pp. 109-119.
[6] A.Fijany, M. A. Jensen, Y. Rahmat-Samii and J. Barhen, "A massively parallel computation strategy for FDTD: time and space parallelism applied to electromagnetics problems," IEEE Trans. Antenna and Propagation, Vol.43, Dec., 1995, pp. 1441-1449.
[7] T. Namiki, "A new FDTD algorithm based on alternating-direction implicit method," IEEE Trans. Microwave Theory Tech., Vol. 47, Oct., 1999, pp. 2003 -2007.
[8] F. Zhen, Z. Chen and J. Zhang, "Toward the development of a three-dimensional unconditionally stable finite-difference time-domain method," IEEE Trans. Microwave Theory Tech., Vol.48, Sept., 2000, pp. 1550-1558.
[9] J.H. Beggs and W. R. Briley, "An implicit characteristic based method for electromagnetics," NASA/TM-2001-210862, May, 2001
[10] G. Sun and C.W. Trueman, "Unconditionally stable Crank-Nicolson scheme for solving the two-dimensional Maxwell's Equations," IEE Electronics Lett., Vol. 39, April, 2003, pp. 595-597.
[11] G. Sun, C. W. Trueman, "Analysis and Numerical Experiments on the Numerical Dispersion of Two-Dimensional ADI-FDTD", IEEE Antennas and Wireless Propaga. Letters, to be published.
[12] J. C. Tannehill, D. A. Anderson, R.H. Pletcher, "*Computational fluid mechanics and heat transfer*," 2nd Ed., Taylor&Francis, Washington, DC, 1997.
[13] Y. Liu, "Fourier analysis of numerical algorithms for the Maxwell's Equations," J. Comput. Phys., Vol. 124, March, 1996, pp. 396-416.

Guilin Sun was born in China in 1962, and received his B.Sc. degree from the Xi'An Institute of Technology in 1982 and his M.Sc. degree from the Beijing Institute of Technology in 1988, respectively, both in optical engineering. From 1988 to 1994 he was an assistant professor at the Xi'an Institute of Technology. From 1994 to 2000 he was an associate professor at the Beijing Institute of Machinery. In 1998-1999 he was a research associate at the University of Southern California, Los Angeles, working on the characterization of E/O polymers used in photonic devices. Currently he is a PhD candidate at Concordia University, Montreal, Canada.

Mr.Sun has published about 70 journal and conference papers in optical engineering and 5 papers on FDTD methods. He has won several awards and honorable titles and his name appears in Marquis "Who's Who in the World", 16th Edition, 1999, New Providence, NJ. Currently his interest is in computational electromagnetics, particularly in new methods of the finite-difference time-domain method in microwave and optical frequencies .

Christopher W. Trueman is a Professor in Electrical and Computer Concordia University, Montreal, Canada. He received the Ph.D. degree from McGill University in 1979 with a thesis on wire-grid modeling aircraft and their HF antennas. His research in Computational Electromagnetics uses moment methods, the finite difference time domain method, and geometrical optics and diffraction. He has worked on EMC problems with standard broadcast antennas and high-voltage power lines, on the radiation patterns of aircraft and ship antennas, on EMC problems among the many antennas carried by aircraft, and on the calculation of the RCS of aircraft and ships. He has studied the near and far fields of cellular telephones operating near the head and hand. Recently he has been concerned indoor propagation of R.F. signals and EMI with medical equipment in hospital environments.